Nuclear Engineering and Technology 53 (2021) 562–571

Contents lists available at ScienceDirect

Nuclear Engineering and Technology

journal homepage: www.elsevier.com/locate/net

Original Article

Towards a physics-based description of intra-granular helium behaviour in oxide fuel for application in fuel performance codes

L. Cognini [a], A. Cechet [a], T. Barani [a], D. Pizzocri [a], P. Van Uffelen [b], L. Luzzi [a, *]

[a] Politecnico di Milano, Department of Energy, Nuclear Engineering Division, via La Masa 34, 20156, Milano, Italy
[b] European Commission, Joint Research Centre, Directorate for Nuclear Safety and Security, P.O. Box 2340, 76125, Karlsruhe, Germany

ARTICLE INFO

Article history:
Received 7 April 2020
Received in revised form
29 June 2020
Accepted 9 July 2020
Available online 26 July 2020

Keywords:
Helium behaviour
Oxide nuclear fuel
Meso-scale modelling
Fuel performance codes

ABSTRACT

In this work, we propose a new mechanistic model for the treatment of helium behaviour which includes the description of helium solubility in oxide fuel. The proposed model has been implemented in SCIANTIX and validated against annealing helium release experiments performed on small doped fuel samples. The overall agreement of the new model with the experimental data is satisfactory, and given the mechanistic formulation of the proposed model, it can be continuously and easily improved by directly including additional phenomena as related experimental data become available.

1. Introduction

A considerable research effort is targeting the improvement of fuel performance codes towards the simulation of fast reactor fuel pin behaviour [1]. In this research framework, helium behaviour plays a significant role compared to UO_2 for application in light water reactors. This is even more true when the considered fuel is devoted to transmutation, presenting consistent initial concentrations of minor actinides and therefore a significant helium production [2].

In order to focus on the modelling of helium behaviour in fuel performance codes, it is useful to make a parallel with the state-of-the-art description of fission gas behaviour. Modelling of fission gas (i.e., xenon and krypton) behaviour in nuclear fuel is typically approached in steps [3]: first, (1) creation by fission reactions, followed by (2) intra-granular evolution [4–7], and lastly by (3) inter-granular evolution [8,9]. A similar step-like modelling approach is herein proposed for the description of helium behaviour. The choice of this fission-gas-inspired model structure, in alternative for example to consider the effective transport of helium along the pellet radius, brings about the possibility to explicitly account for the interaction between helium and fission gas.[1] Moreover, it allows for straight inclusion in fuel performance codes, either by direct implementation or via coupling with meso-scale modules (e.g., SCIANTIX [10,11]). Another feature of a stepwise description of helium behaviour is that each step can be in principle validated (and verified) independently from the others. This is of great importance because of the high uncertainty associated to the model parameters, and justifies the degree of simplification in the current model in which for instance we do not describe point defects. Therefore, it is preferable to assess the behaviour of the model on sub-problems involving a limited number of parameters. Summarizing, the present work should be considered as a first effort in the mechanistic modelling of the complex phenomena linked to the behaviour of helium in nuclear fuel.

The knowledge of the properties that govern the transport of helium and its absorption/release mechanisms is a fundamental step for understanding helium behaviour. For this reason, several separate-effects experiments have been performed in the past in order to investigate and characterize helium diffusivity in nuclear fuel, e.g. Ref. [12–15], providing large uncertainty bands. By carefully reviewing and classifying the data depending on the combination of the technique used to introduce helium in the samples and the micro-structure of the sample itself, clusters ascribed to the different damage level caused to the lattice by the different

* Corresponding author.
E-mail address: lelio.luzzi@polimi.it (L. Luzzi).

[1] In the framework of the INSPYRE H2020 Project [1], a campaign of separate-effects experiments focusing on infusion of a cocktail of noble gases in fresh UO_2 is carried out with the goal of shedding light on the combined behaviour of gases as single-atoms and in precipitated bubbles.

https://doi.org/10.1016/j.net.2020.07.009

techniques appear, and the new correlations obtained are affected by a lower uncertainty [16]. One of the main reasons of the peculiarity of helium behaviour in oxide fuels compared to fission gases comes from its higher solubility [12,13,17]. Complementary to the classification done for the diffusivity [16], Cognini et al. [18], collected and analysed all the experimental data concerning the helium solubility in uranium dioxide and categorized them on the basis of the sample micro-structure, leading to the derivation of two correlations for Henry's constant as a function of temperature. Moreover, several atomistic computer simulations (e.g., Molecular Dynamics – MD and Density Functional Theory – DFT calculations) have been performed to study helium diffusivity and solubility in nuclear fuel [19–24]. These results are a fundamental tool in order to progress in the understanding of the complex phenomena related to inert gas behaviour in such materials [6] and have therefore been included in the plot comparing correlations for diffusivity and solubility (see Fig. 1 and Fig. 2, respectively). In particular, Noirot [24] derived the theoretical value for Henry's constant applying to helium in interstitial positions in UO_2 a method devised to calculate the equilibrium concentration of point defects and gas atoms in the vicinity of a bubble in UO_2. Moreover, Noirot performed 5 different calculations in the range 673–2073K, as reported in Table 1.

The resulting scatter for solubility is larger than the experimental scatter. Therefore, in order to avoid the inclusion of an additional source of uncertainties in the model parameters, we have decided to account, in our analysis, only for the input coming from experimental data, in this early stage of development. Indeed, what still hinders a more intense and direct application of DFT results in fuel performance codes is that, according to the conclusions of the NEA state-of-the-art report [25], the calculations are still open for discussion. Additionally, it is important to underline that the model herein developed is based on parameters derived from experiments mainly with UO_2 fuel, due to the scarcity of data for MOX fuels in literature. An extensive validation of this model also for fast reactors therefore calls for new experiments. These review activities are deemed as fundamental for the development of the herein presented physics-based model.

In this work, we present a model for the intra-granular helium behaviour in UO_2 fuel that represents a first step into the direction of a more mechanistic description, as compared to what is currently in the fuel performance codes. The proposed model is suitable for application in fuel performance codes, and is hence implemented in the fission gas behaviour module SCIANTIX [10] and compared with the current model adopted in the TRANSURANUS performance code [2,26,27]. The proposed model is described in Section 2, together with the physical parameters involved in the model equations. Section 3 presents the main features of the experimental database against which the model calculations are compared, and the results are collected and described in Section 4.

2. Model description

The proposed model aims at a more physics-based description of the helium release and retention mechanisms, which can be directly applied in fuel performance codes. Therefore, in a first step, it does not describe the evolution of point defects. To this end, we extend state-of-the-art models developed for the description of intra-granular fission gas behaviour (such as [5,28,29]) by including the treatment of helium solubility. Besides solubility is not usually considered for xenon and krypton (as discussed and ruled out, e.g., by Lösönen [30]), Veshchunov [4] included it in rate theory models due to its potential contribution at high temperatures. In this work, we propose a description of helium solubility in UO_2 in line with [4,30]. It has been verified that helium solubility in oxide nuclear fuel is linearly proportional to the infusion pressure at a fixed temperature and hence the system He-UO_2 obeys Henry's law [12,13,17,31]:

$$C_S = k_H p \tag{1}$$

where k_H (at m^{-3} MPa^{-1}) is Henry's constant for the He-UO_2 system and C_S (at m^{-3}) is the solubility achieved at a pressure p (MPa).

The inclusion in the model of the mobility of intra-granular helium bubbles has been proposed by Talip et al. [15], based on the observation of helium release rates from doped fuel samples. This model extension follows the generalization of Speight's rate theory model [28] proposed by Van Uffelen et al. [32]. Nevertheless, in this work, we do not include this bubble-diffusivity term due to the scarcity of data available in literature. Indeed, to the best of our knowledge, the only bubble diffusion coefficient available is the one derived in Ref. [15] by fitting the experimental results of helium

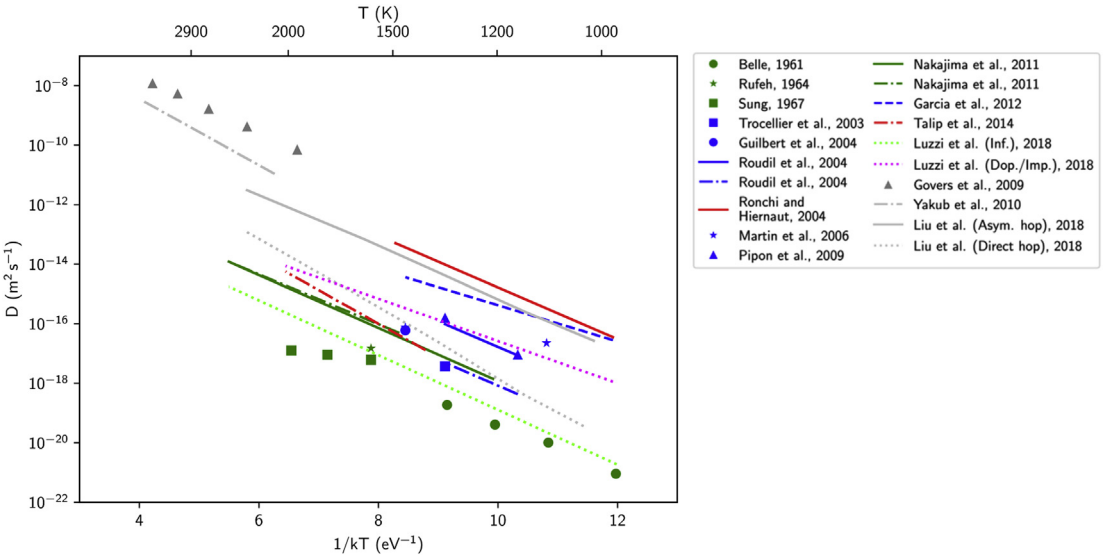

Fig. 1. Plot of experimental helium diffusivity in uranium dioxide as reported in Luzzi et al. [16] to which have been added the results of atomistic simulations (grey [19,20,22]).

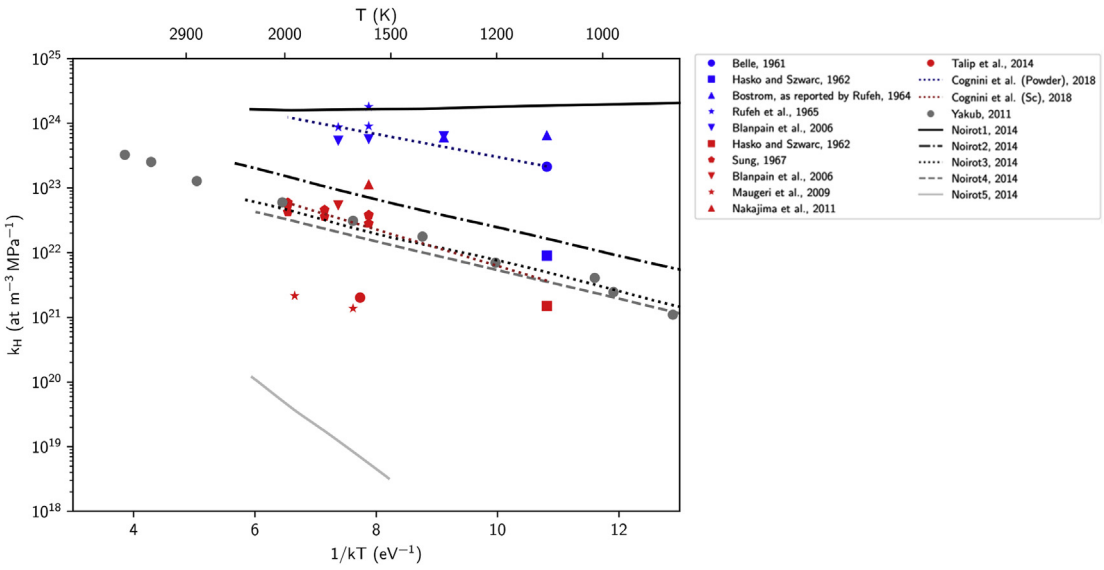

Fig. 2. Plot of experimental helium solubility in uranium dioxide as reported in Cognini et al. [18] to which have been added the results of atomistic simulations (grey [23,24]).

Table 1
Different values of incorporation energies of a helium atom in an interstitial position, E_{inc} and of different activation energies for the diffusion of helium in UO_2, E_j used by Noirot [24] in the atomistic simulations shown in Fig. 2.

Case nr	E_{inc} (eV)	E_j (eV)
1	−0.1	2
2	0.45	0.9
3	0.45	2
4	0.45	2.5
5	1.5	2

release rate during annealing of doped fuel samples. However, we have in the meantime noticed an error in that paper: despite the simulations and consequent plot of results being all correct, the activation energies reported in the equations for single gas atoms diffusion and bubble diffusion have been erroneously interchanged. This clearly does not limit the outcome of the work by Talip and co-authors, but implies that the bubble diffusion coefficient derived in that paper has a lower activation energy compared to the single gas atoms diffusion coefficient, which is questionable as it would imply that bubble diffusion dominates at lower temperatures. For this reason, bubble diffusion has been disregarded in this work. For the same reason, we decided to implement the diffusion coefficient proposed in our previous work [16] that consists in the best fit of all the experimental data available in literature concerning uranium dioxide samples, in which the helium has been introduced by means of infusion. As detailed in Section 3 and 4, this dataset is herein selected as validation base for the proposed model and therefore we apply parameters derived independently.

Summarizing, the proposed model includes single-atoms diffusion (in an equivalent sphere [33]), trapping of single atoms at intra-granular bubbles and irradiation induced re-solution of gas atoms from intra-granular bubbles, helium solubility, and helium production rate. Namely:

$$\begin{aligned}\frac{\partial c}{\partial t} &= S + D\frac{1}{r^2}\frac{\partial}{\partial r}r^2\frac{\partial}{\partial r}c - \beta(c - C_{S,\mathrm{ig}}) + \alpha m \\ \frac{\partial m}{\partial t} &= \beta(c - C_{S,\mathrm{ig}}) - \alpha m\end{aligned} \tag{2}$$

in which r (m) is the radial coordinate along the fuel grain (assumed as spherical) and t (s) is time, c and m (at m^{-3}) are the concentration of helium single-atoms and helium in intra-granular bubbles, respectively, S (at m^{-3} s^{-1}) is the helium production rate,[2] β (s^{-1}) is the trapping rate and α (s^{-1}) is the irradiation-induced re-solution rate, D (m^2 s^{-1}) is the single-atom diffusion coefficient, and $C_{S,\mathrm{ig}}$ (at m^{-3}) is the intra-granular helium solubility. By using Eq. (1), these solubilities are related to the helium pressure in those bubbles, i.e.:

$$C_{S,\mathrm{ig}} = k_H p_{\mathrm{ig}} \tag{3}$$

The boundary conditions assumed for the single-atoms diffusion problem are:

$$\begin{aligned}c(r = a, t) &= C_{S,\mathrm{gb}} = k_H p_{\mathrm{gb}} \\ \frac{\partial}{\partial r}c(r = 0, t) &= 0\end{aligned} \tag{4}$$

where a (m) is the radius of the spherical fuel grain and $C_{S,\mathrm{gb}}$ (at m^{-3}) is the inter-granular helium solubility. As depicted in Eq. (3), this solubility is dependent on the inter-granular pressure which is, in general, a complex data to measure experimentally. A helping hand in understanding the complex phenomena occurring at the grain boundaries could come from atomic scale simulations, as also shown in Ref. [34]. However, in this initial stage of development of the model, we focus on the intra-granular behaviour, comparing with experimental data in which grain boundary phenomena should be less relevant.

Besides the definition of each model parameter appearing in Eq. (2), which is detailed in the following, it is worth noting that the introduction of the solubility calls for the necessity of evaluating the helium pressure within intra- (p_{ig}) and inter-granular bubbles (p_{gb}), as expressed in Eq. (3). This is not trivial since:

- Intra-granular and inter-granular bubbles could have very different size and helium densities, and thus in order to calculate their pressure a wide ranged equation of state is required, or a combination of different equations of state tailored to each bubble population [35].

[2] This term includes ternary fissions, (n,α)-reactions on oxygen, and α-decays.

- The knowledge of solubility of helium at grain boundaries is limited, since the experimental knowledge about solubility in UO_2 derives from infusion in single crystals and powders, with the lack of data available for polycrystalline samples [18]. The estimation of the gas content in inter-granular bubbles is therefore strongly dependent on model assumptions.

In view of these intrinsic limitations in the general application of the model formalized in Eq. (2), we focus on the simplified version of the model applicable to the simulation of *fast annealing* experiments performed in *vacuum conditions* [15]. Despite the loss of generality, this approach allows us to assess the performance of the model with a subset of parameters and to compare its results with the experimental measurements of release rates during annealing in KEMS of doped UO_2 performed by Talip et al. [15] (Sections 3, 4).

In annealing conditions, the irradiation induced re-solution rate is null, $\alpha = 0$, whereas the condition of fast transients allows neglecting the helium production rate, $S \approx 0$, with the average intra-granular concentrations of helium initialized to $c(t) = c_0$ and $m(t) = m_0$. In fact, it is assumed that a bubble population is formed at the first time-step, m_0, and then it evolves during the whole experiment, accordingly to the modelling hypothesis made also in Talip et al. [15]. Moreover, specifically for this case in which the experiments are performed in vacuum (i.e., in the KEMS), the pressure at grain boundaries is assumed to be zero, $p_{gb} \approx 0$, implying by Eq. (3) that $C_{S,gb} = 0$. Under these assumptions and using Henry's law (Eq. (3)), Eq. (2) becomes:

$$\begin{aligned}\frac{\partial c}{\partial t} &= D\frac{1}{r^2}\frac{\partial}{\partial r}r^2\frac{\partial}{\partial r}c - \beta\left(c - k_H p_{ig}\right) = D\frac{1}{r^2}\frac{\partial}{\partial r}r^2\frac{\partial}{\partial r}c - \beta c + \beta k_H p_{ig}\\ \frac{\partial m}{\partial t} &= \beta\left(c - k_H p_{ig}\right) = \beta c - \beta k_H p_{ig}\end{aligned} \tag{5}$$

in which the term $\beta k_H p_{ig}$ represents thermal re-solution.

By using the classic trapping rate by Ham [36]

$$\beta = 4\pi D R_{ig} N_{ig} \tag{6}$$

where R_{ig} (m) is the radius of intra-granular bubbles and N_{ig} (at m^{-3}) is the intra-granular bubble density, and using the Van Brutzel et al. [35] equation of state for the intra-granular bubble pressure p_{ig} (Pa)[3]

$$p_{ig} = \frac{kT}{V_{at}}Z \tag{7}$$

where k ($J\,K^{-1}$) is the Boltzmann's constant, T (K) the temperature, Z the compressibility factor, and V_{at} the atomic specific volume, i.e., $V_{at} = V_{ig}/n_{He}$, with V_{ig} (m^3) being the intra-granular bubble volume and n_{He} (at) being the number of atoms per bubble. We can write:

$$\beta k_H p_{ig} = 4\pi D R_{ig} N_{ig} k_H \frac{kTZn_{He}}{V_{ig}} = \left(4\pi D R_{ig} k_H \frac{kTZ}{V_{ig}}\right)\left(n_{He}N_{ig}\right) := \gamma m \tag{8}$$

where γ (s^{-1}) is interpreted as a thermal re-solution rate.[4] With this notation Eq. (5) can be written as:

$$\begin{aligned}\frac{\partial c}{\partial t} &= D\frac{1}{r^2}\frac{\partial}{\partial r}r^2\frac{\partial}{\partial r}c - \beta c + \gamma m\\ \frac{\partial m}{\partial t} &= \beta c - \gamma m\end{aligned} \tag{9}$$

which is formally the homogeneous form (i.e., with no source term) of the system studied by Speight [28].

As for the model parameters to be used in Eq. (9), we adopt Ham's trapping rate β [36] (Eq. (6)), the thermal re-solution rate γ defined by Eq. (8), and the diffusion coefficient D by Luzzi et al. [16], recommended for infused samples[5] and valid in the temperature range 968–2110 K, i.e.:

$$D\left(m^2 s^{-1}\right) = 2.0\ 10^{-10}\exp(-2.12\ (eV)/kT) \tag{10}$$

The Henry's constant is selected after the review of Cognini et al. [18]. We use the relation reported for single crystals and valid in the temperature range of 1073–1773 K, since Eq. (9) describes the solubility of helium *within* a fuel grain

$$k_H\left(\text{at}\ m^{-3}MPa^{-1}\right) = 4.1\ 10^{24}\exp(-0.65\ (eV)/kT) \tag{11}$$

Moreover, in the attempt to account for the grain changings that could have an important effect on the evolution of helium content, the grain growth and the related grain boundary sweeping have been considered in our model.

For the sake of comparison, we report the model for helium behaviour[6] currently implemented in TRANSURANUS [2]. This model includes the treatment of intra-granular helium diffusion with an effective diffusivity D_{eff} acting on the total helium concentration, in line with [28,32]. The diffusion coefficient is based on the best-estimate correlation derived by Federici et al. [27]. [7] The governing equation is:

$$\frac{\partial(c+m)}{\partial t} = D_{eff}\frac{1}{r^2}\frac{\partial}{\partial r}r^2\frac{\partial}{\partial r}(c+m) + S \tag{12}$$

with the source rate being calculated from the TUBRNP depletion module [2,37]. As for the inter-granular helium behaviour, the model assumes that above 800°C all the gas reaching the grain boundaries is released, whereas at lower temperatures the helium is trapped at the grain boundaries up to a certain saturation value.

Both the new model (Eq. (2)) and the current TRANSURANUS one (Eq. (12)) have been implemented in SCIANTIX [10,11,38].

[3] For the sake of completeness, the equation of state is here summarized: $p_{ig} = kTZ/V_{at}$, $Z = (1+y+y^2-y^3)/(1-y)^3$, $y = \pi d^3/6V_{at}$, with V_{at} (m^3) = 7.8 10^{-30} under the approximation of saturated nanobubbles, and d being the hard-sphere diameter given by d (m) = 2.973 10^{-10} [0.8414–0.05 ln(T (K)/10.985)]. The assumption of constant V_{at} is in line with the required complexity of the model but is not supported by any physical interpretation. At the cost of increasing the complexity of the model (in terms of number of equations and of parameters), one could include the description of the evolution of point defects allowing for a more physical description of vacancy absorption at intra-granular bubbles. This development exceeds the scope of the present work, but is deemed relevant considering that the lattice damage accumulated in the samples considered (0.04 dpa at very low temperature) is expected to lead to the buildup of a non-negligible vacancy concentration.

[4] This definition of the thermal re-solution is dependent on the choice of the equation of state for intra-granular helium bubbles. Different equation of states will imply different formulas for γ [30].

[5] The sample was estimated to have 0.04 dpa (displacements per atom) at the time it was examined, far from typical values reached in irradiated fuel.

[6] In TRANSURANUS, also a model describing the absorption of helium from the rod free volume is present. This model is out of the scope of this work and is therefore not discussed.

[7] Alternatively, a lower [27] or an upper [43] bound of the data can be selected.

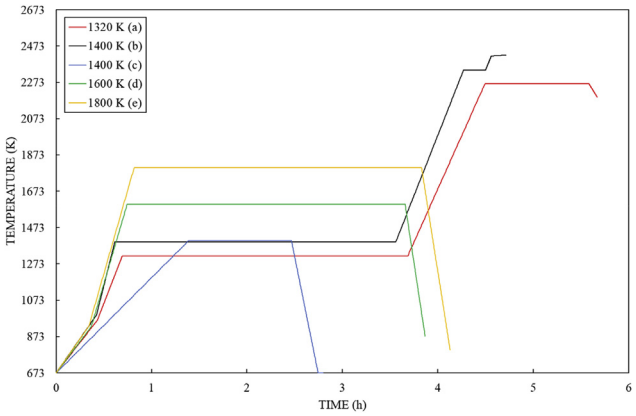

Fig. 3. Temperature histories of the annealing experiments considered [15].

3. Description of the annealing experiments and simulation set-up

The goal of the separate-effects experiments performed by Talip et al. [15] is to investigate the helium release from UO_2 samples doped with 0.1 wt% of additive containing 66.7 wt% of $^{238}PuO_2$, aged 15 years in a glovebox with inert atmosphere (N_2). The samples have been subject to helium desorption experiments performed in a Knudsen Effusion Mass Spectrometry (KEMS) system connected to a Quantitative GAs MEasurement Set-up (Q-GAMES). In this technique, the helium released from the samples during the annealing is collected, purified and quantitatively measured by comparison with a known spike of gas [39].

The five annealing temperature histories considered in this work (see Fig. 3) are characterized by a heat up step (around 30 min with 10–30 K min^{-1}), followed by a holding at the annealing temperature (for 1–3 h). In three out of five annealing histories, the temperature is decreased after the plateau, while in two histories there is a second heat up phase up to 2200–2300 K. For each temperature history, two figures of merit have been analysed, namely: the helium fractional release and the helium release rate. The helium fractional release is measured up to the end of the annealing plateau, while the helium release rate is measured continuously to the end of the annealing history (i.e., for two cases, up to 2200–2300 K).

The experimental measurements are supported by SEM images [15] allowing to estimate the population of helium bubbles in the sample before it experiences the annealing history. In line with Talip et al. [15] we assume an initial concentration of helium single-gas atoms $c_0 = 1.6\ 10^{24}$ at m^{-3} and a helium concentration trapped in intra-granular bubbles of $m_0 = 8.3\ 10^{22}$ at m^{-3}. Based on the measurement of bubble size in the order of 1–2 nm, a bubble density of 400 atoms per bubbles is assumed, resulting in a number density of $N_{ig} = 2.08\ 10^{20}$ bub m^{-3} intra-granular bubbles. In detail, we assume that the choice of considering 400 helium atoms per bubble in Talip et al. comes from the ratio V_{ig}/V_{He} where V_{ig} is the volume of intra-granular bubbles considered as spheres with a radius of 1 nm and V_{He} is the atomic volume of helium.

In recognition of the impact of the grain size, a (m), in the evolution of helium behaviour (e.g., affecting the diffusion rate D/a^2 (s^{-1}) and eventually sweeping the intra-granular helium concentration by grain growth, providing an additional release contribution) Talip et al. [15] measured the grain size before and after the annealing experiments, reporting a general trend of strong grain growth. In order to attempt to account for this effect, the grain growth and the consequent grain boundary sweeping have been included in SCIANTIX: we use the Van Uffelen et al. grain growth model [40] and the same model present in TRANSURANUS for the swept volume fraction [41].

4. Discussion of results

Fig. 4 reports the total concentration of helium, as single atoms (c_0) and bubbles (m_0), used for the initialization of the helium behaviour model in SCIANTIX (see Section 2)[8] and their evolution as function of the annealing time, together with the helium released, for the cases at 1320 K (on the left) and 1800 K (on the right). As it appears from Fig. 4, the curves are qualitatively similar in both cases. In fact, for what concerns the annealing temperature history at lower temperature (Fig. 3 case (a) and Fig. 4, left panels), during the first 20 min, m quickly goes to zero, while c increases up to an equilibrium value and, in correspondence to the plateau (at 1320 K) starts to decrease slowly. Once the plateau finishes, the temperature rises again, and c decreases more quickly reaching the value $8.17\ 10^{21}$, after almost 6 h from the beginning of the annealing history. Likewise, it happens for the annealing temperature history at higher temperature (Fig. 3 case (e) and Fig. 4, right panels). During the first 15 min, m quickly goes to zero, while c increases up to a stable value and then it decreases during the annealing down to $2.92\ 10^{23}$, after 4 h from the beginning of the experiment. From the comparison of these two cases, it emerges that at the beginning of the annealing histories, the initial single helium atoms in solution in the matrix (c) increase at the expense of the bubble concentration (m) due to the thermal re-solution that is dominant compared to the trapping, as explained in more detail below. In addition, also regarding to the helium released from the samples (the yellow curves in Fig. 4), the behaviour results qualitatively similar with an increase of the release correspondent to a heat up step of the annealing temperatures.

Figs. 5 and 6 collect the results of the SCIANTIX simulations using both the new helium behaviour model and the current model available in TRANSURANUS. The simulation results are compared with the experimental release in terms of helium fractional release (Fig. 5) and of helium release rate (Fig. 6).

From the observation of Fig. 5, it appears that both the current TRANSURANUS model and the new proposed model have a satisfactory agreement with the experimental results. The mean square errors calculated between the simulation results and the experimental data are reported in Table 2, and quantitatively confirm this observation. Despite adopting an effective treatment of helium diffusivity, TRANSURANUS model catches both the kinetics and the integral values of the helium release remarkably well, in all the range of considered annealing temperatures.

It should be added that the effective diffusivity by Federici et al. [27] is the *only* parameter considered in the model of TRANSURANUS, since the grain-boundary release temperature threshold and the grain-boundary retention [2] are turned off to represent the vacuum conditions in which the annealing is performed. The effective diffusion coefficient D_{eff} proposed by Federici et al. represents (in the model of TRANSURANUS) a combination of the single-atom diffusivity D, the trapping rate β, and the thermal and irradiation-induced re-solution rate γ and α, i.e., $D_{eff} = (\alpha + \gamma)/(\beta + \alpha + \gamma)\ D$, whereas the new mechanistic model proposed describes each of these parameters separately. Up to a certain degree, it is expected that adding physics-based parameters with considerable

[8] Besides the other model parameters (helium diffusivity and solubility) described in Section 2, we briefly recall that since the annealing is performed in vacuum conditions, we assume zero retention of helium at the grain boundaries. Moreover, we neglect the source term because of the short duration of the annealing histories.

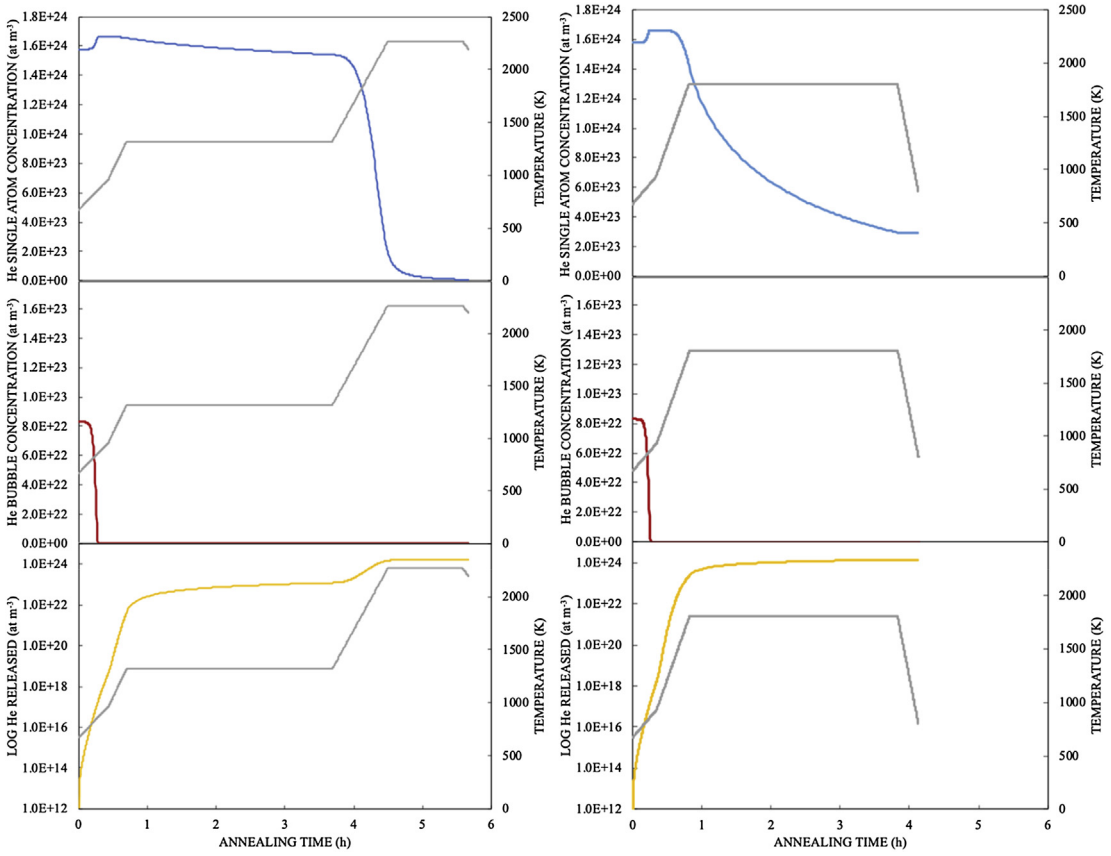

Fig. 4. Evolution of the helium concentration in the samples as single atoms (blue line) and bubbles (red line) as a function of the annealing time for the temperature histories at 1320 K (left panels: case (a) in Fig. 3), and 1800 K (right panels: case (e) in Fig. 3). The yellow curves represent, in logarithmic scale, the helium released from the two samples, respectively. (For interpretation of the references to colour in this figure legend, the reader is referred to the Web version of this article.)

uncertainty [16,18,33,42] results in a limited predictive capability of the model itself. Nevertheless, it is fair to say that the combination of the physics-based parameters should attempt to reproduce the effective diffusion coefficient by Federici et al., in view of its (*i*) capability in reproducing experimental data (Fig. 5), and it (*ii*) being the best-estimate fit of several experimental diffusivity measurements [27]. This represents a development target for future work on mechanistic models.

Fig. 6 reports the comparison of the simulation results with the experimental data in terms of helium release as function of temperature. For the annealing histories with the first plateau at 1320 K (Fig. 6a) and 1400 K (Fig. 6b) two distinct peaks can be observed. Beside the relatively poor quantitative agreement, both the new proposed model and the TRANSURANUS model correctly predict the onset of both release-rate peaks in this release. This is particularly important since this two-peaked release-rate evolution has been ascribed to the mobility of helium intra-granular bubbles [15], which is not considered in the herein analysed models.[9] In the present description, for these two cases, the second peak is caused by the rise in temperature of the annealing transient (Fig. 3) and the consequent (*i*) increase in the diffusion rate of helium towards the grain boundaries, together with (*ii*) a strong grain growth becoming significant above 2000 K and the associated grain boundary sweeping. It is worth noting that grain boundary sweeping plays a major role in the formation of the second peak and therefore it is crucial to include this effect (Fig. 7). In the calculations, the supplementary fractional release term from the grains to the grain boundaries is approximated by the volume fraction of the fuel swept by the moving boundaries during each time step.

Fig. 6e shows the highest temperature plateau analysed, i.e., the annealing history at 1800 K (Fig. 3). This case shows two release-rate peaks, with an almost 100% helium fractional release (Fig. 5e). Both peaks are observed during the heat up phase of the annealing. This behaviour indeed suggests the activation of a second release mechanism with an activation energy higher than that of either the diffusivity of single atoms by Luzzi et al. [16] or the effective diffusivity by Federici et al. [27]. The new proposed mechanistic model is unable to catch this second peak at higher temperature, despite the additional parameters compared to the current TRANSURANUS model. With suited parameters, the model itself could explain a two-peak release behaviour. A possible mechanism could be: (*i*) first the diffusion of single atoms activates, leading to trapping of gas at intra-granular bubbles and to diffusion towards the grain boundaries – i.e., causing the first peak of release, (*ii*) second, at higher temperature, the thermal re-solution becomes dominant compared to trapping and hence helium is re-solved in the matrix and becomes available for diffusion – i.e., the second peak. Nevertheless, this hypothetical evolution of intra-granular helium is not predicted by the model, since the thermal re-solution is always dominant compared to the trapping rate, also at lower temperatures, i.e., at the beginning of the annealing tests.

[9] It could be said that since the description by Federici et al. is *effective*, it includes already also the mobility of intra-granular bubbles. Nevertheless, the coefficient proposed by Federici et al. is Arrhenius-like, i.e., $D_{eff} = D_0 \exp(-E/kT)$ with E being the activation energy, 1/kT the Boltzmann's factor and D_0 a pre-exponential, while it is expected that the motion of intra-granular bubbles should have a specific activation energy, different from that of single atoms.

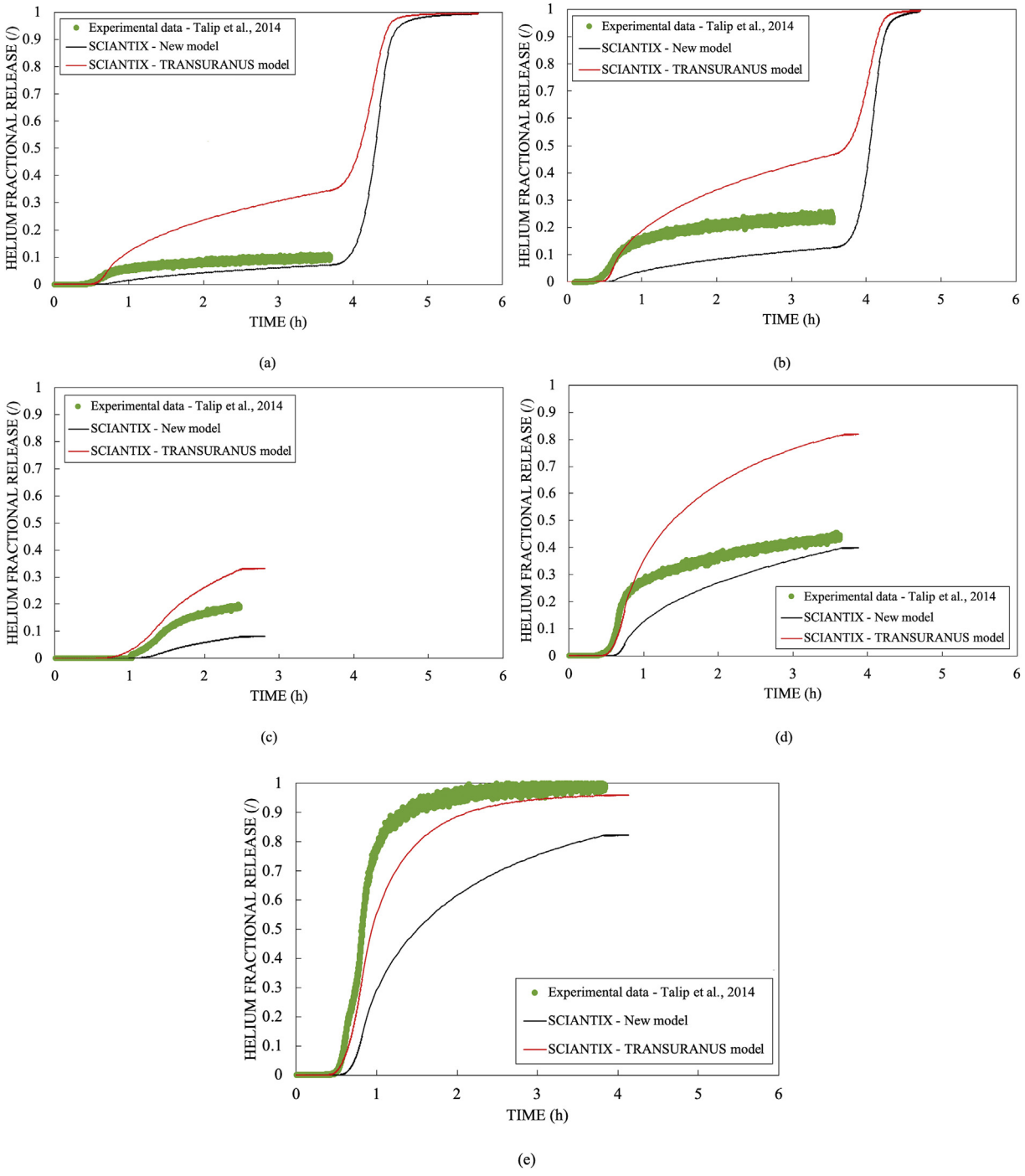

Fig. 5. Comparison of SCIANTIX results (new helium model and current TRANSURANUS model) with experimental helium fractional release from Ref. [15]. Each subfigure corresponds to an annealing history which is referred to by the temperature of its first plateau, respectively (a) 1320 K, (b) 1400 K, (c) 1400 K, (d) 1600 K, and (e) 1800 K (see Fig. 3).

In detail, writing Eq. (10) and Eq. (11) as $D = D_0\exp(-E_D/kT)$ and $k_H = k_{H_0}\exp(-E_{k_H}/kT)$, respectively, we can also express the trapping rate β and the thermal re-solution rate γ as Arrhenius-like:

$$\beta = 4\pi D_0 R_{ig} N_{ig} \exp(-E_D/kT) = \beta_0 \exp(-E_D/kT) \quad (13)$$

with $\beta_0 = 4\pi D_0 R_{ig} N_{ig}$ and

$$\gamma = 4\pi D_0 R_{ig} k_{H0} \frac{kTZ}{V_{ig}} \exp(-(E_D + E_{k_H})/kT) = \gamma_0 \exp(-(E_D + E_{k_H})/kT) \quad (14)$$

with $\gamma_0 = 4\pi D_0 R_{ig} k_{H0} \frac{kTZ}{V_{ig}}$.

Comparing Eq. (13) and Eq. (14), it is evident that the activation energy of the thermal re-solution is always slightly higher than the activation energy of the trapping, suggesting a prevalence of trapping over the thermal re-solution at low temperatures. However, it

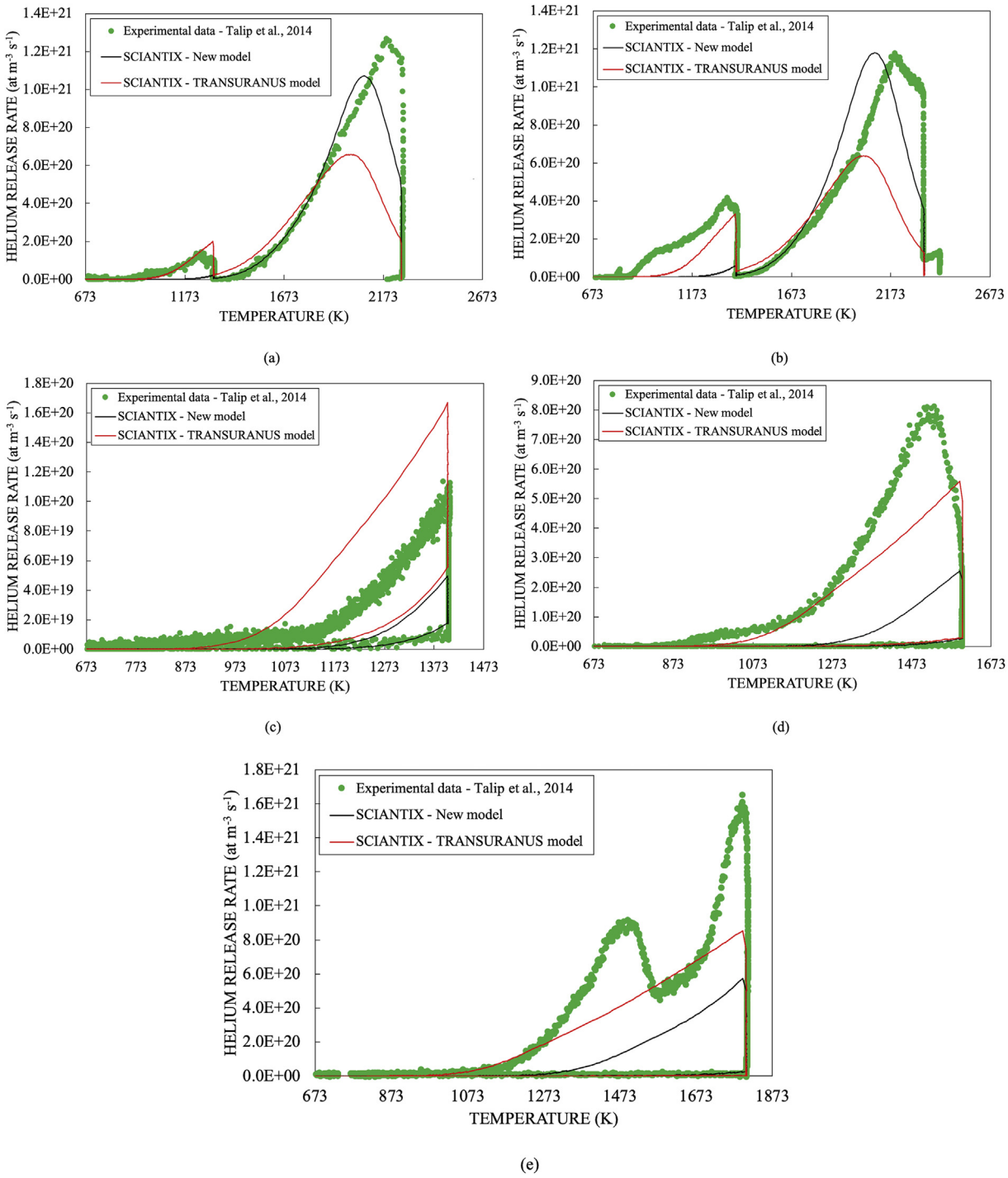

Fig. 6. Comparison of SCIANTIX results (new helium model and current TRANSURANUS model) with experimental helium release rate from Ref. [15]. Each subfigure corresponds to an annealing history which is referred to by the temperature of its first plateau, respectively (a) 1320 K, (b) 1400 K, (c) 1400 K, (d) 1600 K, and (e) 1800 K (see Fig. 3).

is the opposite, due to the great difference in the pre-exponential factors, as shown for T = 1800 K in the following calculation

$$\frac{\gamma_0}{\beta_0} = \frac{k_{H_0} kTZ}{V_{ig} N_{ig}} \approx 10^{11} \tag{15}$$

Consequently, the trapping mechanism results extremely weak and once all the helium initially contained in the intra-granular bubbles is re-solved into the matrix, it diffuses (at higher temperature) towards the grain boundaries, resulting in a single peak of release.

Summarizing, the discrepancies shown in Figs. 5 and 6 between the results simulated in SCIANTIX and the ones obtained with TRANSURANUS are mainly related to the different diffusion coefficient used: the one derived by Luzzi et al. [16] and the effective diffusion coefficient proposed by Federici et al. [27], respectively. Moreover, the limited predictive capability of the helium release rate at high temperature by the new proposed model can be ascribed to:

Table 2
Validation metric (mean square error) for the comparison of the simulation results with the experimental data by Talip et al. [15] in terms of helium fractional release (see Figs. 3 and 5). Lower values of the validation metric correspond to a better agreement.

Annealing history	Current TRANSURANUS model	New mechanistic model
1320 K (a)	1.48	0.74
1400 K (b)	0.64	0.76
1400 K (c)	0.76	0.69
1600 K (d)	0.62	0.64
1800 K (e)	0.28	0.57

- The considerable uncertainty associated to the model parameters, especially to the temperature dependence of the trapping rate and of the thermal re-solution rate.
- The lack of representation of another release mechanism, e.g., intra-granular bubble mobility, a degree of grain-boundary retention, pipe diffusion along grain boundaries, evaporation at higher temperatures with associated stoichiometry variations, ect. Nevertheless, in view of the results on helium release observed in Fig. 3 of Hiernaut et al. [44], it seems that evaporation only plays a role above 1700 K and does not play a dominant role in helium release, in contrast with the release of other fission products.

A combination of these two issues could also be the case, but given the lack of more experimental data, however, it seems hard to justify introducing additional parameters and equations at this stage of the model development. If the poor characterization of the model parameters is responsible of the non-satisfactory agreement with the experimental data, it appears that the most critical parameter is the thermal re-solution. This can be deducted from the fact that the activation of the diffusivity proposed by Luzzi et al. [16] is similar to that proposed by Federici et al. [27]. Consequently both models considered are able to correctly predict the onset of the first peak, whereas the thermal re-solution contains both the equation of state of intra-granular bubbles (which is not trivial to address [33]) and Henry's constant, which is also poorly characterised experimentally [18]. Despite the big impact of the grain growth in these experiments, the model for grain growth applied both in Ref. [15] and in this paper is not able to reproduce properly all the measured values reported by Talip et al. [15], especially for the annealing histories at the lower temperatures. This could be due to the characteristic of these separate-effects experiments, in which only helium, among the fission gases, is considered. It is also important to keep in mind the uncertainty on the measured average grain growth, even in un-irradiated materials. More experimental data would therefore be required, in which factors that play an important role on grain growth (e.g., stoichiometry variations) are measured (and controlled).

5. Conclusions

In this work, we compared simulation results of helium behaviour and experimental data. Two models are considered, i.e., the current model available in TRANSURANUS and a new, more mechanistic model. Both models are implemented in SCIANTIX, which can be applied for the design and interpretation of separate-effects experiments. The experimental data considered are annealing tests performed in vacuum conditions at different temperatures.

The agreement between the results of the new mechanistic model and the experimental data is overall encouraging and proves that it is equivalent with the current semi-empirical model in TRANSURANUS. The remaining differences have been ascribed mostly to a poor characterisation of some model parameters. In particular, the thermal re-solution represents still an uncertain term, especially for specific experimental conditions such as those considered here. The re-solution contains both the equation of state of intra-granular bubbles and the Henry's constant, for which only few experimental data are available in the open literature. To address this issue, future experiments are planned, e.g., in the frame of the INSPYRE Project concerning the solubility (and diffusivity) of helium in UO_2 and in MOX fuel, whose results will be tested in the presented mechanistic model thus also aiming to simulate the behaviour of fast reactor fuel. In this respect, it will also be very important to analyse the potential impact of stoichiometry variations on the model parameters of helium, since it is known to have a strong impact on fission product behaviour in general. In parallel to the experimental work, the analysis of the point defects evolution will also be required as pointed out in the analysis of the experiments considered here.

Given the mechanistic formulation of the new proposed model, it will be possible to include directly new equations and parameters as they become available, either from lower-length scale calculations or from dedicated experiments. This direction of future development is intended at tackling one of the main model limitations, i.e., the non-explicit consideration of the evolution of point defects. Furthermore, the mechanistic approach, which is even

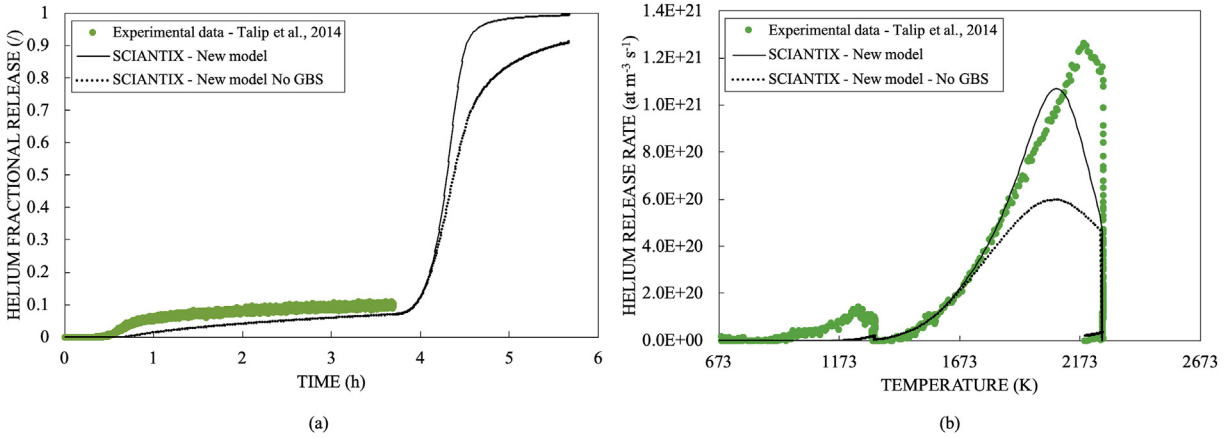

Fig. 7. Comparison of SCIANTIX results (new helium model), including and excluding grain boundary sweeping (GBS), with experimental data from Ref. [15]. Each subfigure corresponds to the 1320 K temperature history, respectively (a) fractional helium release and (b) helium release rate.

more extensively adopted in the MFPR-F code for example, is suitable to combine the models for the inert fission gases and helium in irradiated fuels that are integrated in SCIANTIX and can be applied in fuel performance codes.

Declaration of competing interest

The authors declare that they have no known competing financial interests or personal relationships that could have appeared to influence the work reported in this paper.

Acknowledgements

This research has received funding from the Euratom research and training programme 2014-2018 through the INSPYRE Project under Grant Agreement No. 754329.

References

[1] M. Bertolus, INSPYRE: investigations supporting MOX fuel licensing in ESNII prototype reactors [Online]. Available, http://www.eera-jpnm.eu/inspyre/, 2017.
[2] P. Botazzoli, Helium Production and Behaviour in LWR Oxide Nuclear Fuels, PhD Thesis, Politec. di Milano, Italy, 2011. January.
[3] H. Matzke, Gas release mechanisms in UO_2 - a critical review, Radiat. Eff. 53 (1980) 219–242.
[4] M.S. Veshchunov, On the theory of fission gas bubble evolution in irradiated UO_2 fuel, J. Nucl. Mater. 277 (2000) 67–81.
[5] D.R. Olander, D. Wongsawaeng, Re-solution of fission gas – a review: Part I. Intragranular bubbles, J. Nucl. Mater. 354 (1–3) (2006) 94–109.
[6] M. Tonks, et al., Unit mechanisms of fission gas release: current understanding and future needs, J. Nucl. Mater. 504 (2018) 300–317.
[7] J. Rest, et al., Fission gas release from UO_2 nuclear fuel: a review, J. Nucl. Mater. 513 (2019) 310–345.
[8] R.J. White, The development of grain-face porosity in irradiated oxide fuel, J. Nucl. Mater. 325 (2004) 61–77.
[9] T. Barani, et al., Analysis of transient fission gas behaviour in oxide fuel using BISON and TRANSURANUS, J. Nucl. Mater. 486 (2017).
[10] D. Pizzocri, T. Barani, L. Luzzi, SCIANTIX: a new open source multi-scale code for fission gas behaviour modelling designed for nuclear fuel performance codes, J. Nucl. Mater. 532 (2020).
[11] D. Pizzocri, T. Barani, L. Luzzi, SCIANTIX code, Online Repos.. [Online]. Available, https://gitlab.com/poliminrg/sciantix. Accessed: 04-Oct-2019.
[12] P. Sung, Equilibrium Solubility and Diffusivity of Helium in Single-Crystal Uranium Dioxide, University of Washington, 1967. PhD Thesis.
[13] K. Nakajima, H. Serizawa, N. Shirasu, Y. Haga, Y. Arai, The solubility and diffusion coefficient of helium in uranium dioxide, J. Nucl. Mater. 419 (1–3) (2011) 272–280.
[14] G. Martin, et al., A NRA study of temperature and heavy ion irradiation effects on helium migration in sintered uranium dioxide, J. Nucl. Mater. 357 (1–3) (2006) 198–205.
[15] Z. Talip, et al., Thermal diffusion of helium in ^{238}Pu-doped UO_2, J. Nucl. Mater. 445 (1–3) (2014) 117–127.
[16] L. Luzzi, et al., Helium diffusivity in oxide nuclear fuel: critical data analysis and new correlations, Nucl. Eng. Des. 330 (2018).
[17] E. Maugeri, et al., Helium solubility and behaviour in uranium dioxide, J. Nucl. Mater. 385 (2) (2009) 461–466.
[18] L. Cognini, et al., "Helium solubility in oxide nuclear fuel: derivation of new correlations for Henry's constant, Nucl. Eng. Des. 340 (April) (2018) 240–244.
[19] E. Yakub, et al., Diffusion of helium in non-stoichiometric uranium dioxide, J. Nucl. Mater. 400 (2010) 189–195.
[20] K. Govers, et al., Molecular dynamics simulation of helium and oxygen diffusion in $UO_{2\pm x}$, J. Nucl. Mater. 395 (2009) 131–139.
[21] Y. Yun, et al., Theory of He trapping, diffusion, and clustering in UO_2, J. Nucl. Mater. 385 (2009) 510–516.
[22] X.-Y. Liu, et al., Revisiting the diffusion mechanism of helium in UO_2: a DFT+U study, J. Nucl. Mater. 498 (2018) 373–377.
[23] E. Yakub, et al., Helium solubility in uranium dioxide from molecular dynamics simulations, J. Nucl. Mater. 414 (2011) 83–87.
[24] L. Noirot, A method to calculate equilibrium concentrations of gas and defects in the vicinity of an over-pressured bubble in UO_2, J. Nucl. Mater. 447 (2014) 166–178.
[25] reportState-of-the-Art Report on Multi-Scale Modelling of Nuclear Fuels", Nuclear Science, NEA/NSC/R(2015)vol. 5, 2015.
[26] K. Lassmann, TRANSURANUS: a fuel rod analysis code ready for use, J. Nucl. Mater. 188 (C) (1992) 295–302.
[27] E. Federici, A. Courcelle, P. Blanpain, H. Cognon, Helium production and behavior in nuclear oxide fuels during irradiation in LWR, in: Proceedings of the 2007 International LWR Fuel Performance Meeting, San Francisco, California, 2007, pp. 664–673.
[28] M.V. Speight, A calculation on the migration of fission gas in material exhibiting precipitation and Re-solution of gas atoms under irradiation, Nucl. Sci. Eng. 37 (2) (1969) 180–185.
[29] D. Pizzocri, et al., A model describing intra-granular fission gas behaviour in oxide fuel for advanced engineering tools, J. Nucl. Mater. 502 (2018).
[30] P. Lösönen, On the behaviour of intragranular fission gas in UO_2 fuel, J. Nucl. Mater. 280 (1) (2000) 56–72.
[31] F. Rufeh, et al., The solubility of helium in uranium dioxide, Nucl. Sci. Eng. 23 (1965) 335–338.
[32] P. van Uffelen, G. Pastore, V. di Marcello, L. Luzzi, Multiscale modelling for the fission gas behaviour in the TRANSURANUS Code, Nucl. Eng. Technol. 43 (6) (2011) 477–488.
[33] A.M. Booth, A Method of Calculating Fission Gas Diffusion from UO_2 Fuel and its Application to the X-2-F Loop Test, 1957.
[34] C.O.T. Galvin, Pipe and grain boundary diffusion of He in UO_2, J. Phys. Condens. Matter 28 (2016).
[35] L. Van Brutzel, A. Chartier, A new equation of state for helium nanobubbles embedded in UO_2 matrix calculated via molucelar dynamics simulations, J. Nucl. Mater. 518 (2019) 431–439.
[36] F.S. Ham, Theory of diffusion-limited precipitation, J. Phys. Chem. Solid. 6 (4) (1958) 335–351.
[37] K. Lassmann, C. O'Carroll, J. van de Laar, C.T. Walker, The radial distribution of plutonium in high burnup UO_2 fuels, J. Nucl. Mater. 208 (3) (Feb. 1994) 223–231.
[38] D. Pizzocri, T. Barani, L. Luzzi, Coupling of TRANSURANUS with the SCIANTIX fission gas behaviour module, in: International Workshop "Towards Nuclear Fuel Modelling in the Various Reactor Types across Europe,", 2019.
[39] J.-Y. Colle, et al., A mass spectrometry method for quantitative and kinetic analysis of gas release from nuclear materials and its application to helium desorption from UO_2 and fission gas release from irradiated fuel, J. Nucl. Sci. Technol. 51 (5) (2014) 700–711.
[40] P. Van Uffelen, et al., An experimental study of grain growth in mixed oxide samples with various microstructures and plutonium concentrations, J. Nucl. Mater. 434 (1–3) (2013) 287–290.
[41] K. Lassmann, A. Schubert, P. Van Uffelen, C. Gyori, J. Van De Laar, TRANSURANUS Handbook, Karlsruhe, Germany, 2014.
[42] D. Pizzocri, et al., Review of Available Models and Progress on the Sub-models Dealing with the Intra- and Intergranular Inert Gas Behaviour, 2019.
[43] C. Ronchi, J.P. Hiernaut, Helium diffusion in uranium and plutonium oxides, J. Nucl. Mater. 325 (2004) 1–12.
[44] J.P. Hiernaut, et al., Fission product release and microstructure changes during laboratory annealing of a very high burn-up fuel specimen, J. Nucl. Mater. 377 (2008) 313–324.